

# CLUSTERING IN DEEP (SUBMILLIMETRE) SURVEYS

ENRIQUE GAZTAÑAGA & DAVID H. HUGHES

*Instituto Nacional de Astrofísica, Óptica y Electrónica (INAOE),  
Luis Enrique Erro 1, Tonantzintla, Cholula, 78840 Puebla, Mexico*

Hughes & Gaztañaga (2001, see article in these proceedings) have presented realistic simulations to address key issues confronting existing and forthcoming submm surveys. An important aspect illustrated by the simulations is the effect induced on the counts by the sampling variance of the large-scale galaxy clustering. We find factors of up to  $\sim 2-4$  variation (from the mean) in the extracted counts from deep surveys identical in area ( $\sim 6 \text{ arcmin}^2$ ) to the SCUBA surveys of the Hubble Deep Fields (HDF) <sup>4</sup>. Here we present a recipe to model the expected degree of clustering as a function of sample area and redshift.

## 1 A model for the angular clustering

Fig.1 shows fluctuations in the galaxy counts as measured in the APM Galaxy Survey <sup>5</sup>. Symbols with errorbars show the square root of the variance  $\bar{w}_2(\theta)$ , *e.g.*  $\Delta N/N \equiv \sqrt{\bar{w}_2}$ , measured in squared cells of area  $A \equiv \theta^2$ . The data can be described by a power law:

$$\Delta N/N \equiv \sqrt{\bar{w}_2} \simeq (A/A_0)^\beta$$

with  $A_0 \simeq 7.6 \times 10^{-5} \text{ sq.deg.}$  and  $\beta \simeq -0.175$ , for  $A < 2.7 \text{ sq. deg.}$  For larger areas there is an exponential cut-off with a characteristic scale of  $A_c \sim 110 \text{ sq. deg.}$  The complete model is represented by:

$$\frac{\Delta N}{N} \simeq (A/A_0)^\beta \exp[-A/A_c], \quad (1)$$

and is shown as a solid curve in Fig.1.

## 2 Shot-noise

The effects of shot-noise on the counts, *e.g.* due to the small number of sources in the sample, is easy to quantify. If the mean number density of sources at a given flux is  $\mathcal{N}$ , then the number of sources in a sample of area  $A$  is:  $N = A\mathcal{N}$ . The total variance on such area is:

$$\bar{w}_2^{total} = \bar{w}_2 + \frac{1}{N}, \quad (2)$$

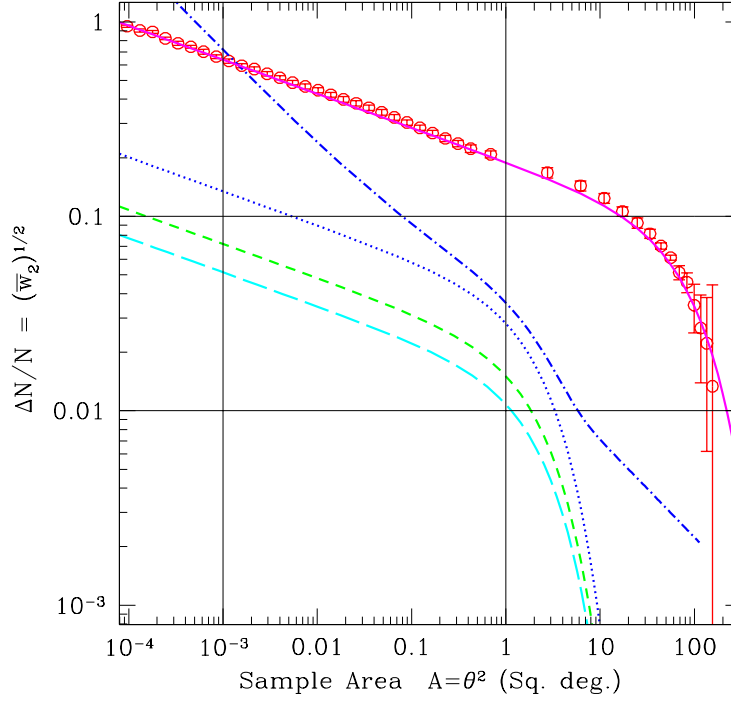


Figure 1. Mean square root deviation in number counts as a function of the sampled area in the sky. Circles with error-bars correspond to counts in square cells of different areas measured in the APM survey. The solid curve shows the model in Eq.[1]. The predicted fluctuations, scaled to a depth of  $\mathcal{D} \simeq 2500h^{-1}\text{Mpc}$  ( $z \sim 3$ ), are shown for different clustering evolution models: fixed in co-moving coordinates (dotted line), stable clustering (dashed lines) and linear theory (long-dashed lines). The dot-dashed line includes the shot-noise contribution for a surface density of 2000 sources/sq. deg.

where  $\bar{w}_2$  is the intrinsic variance (in the case of high density) <sup>1</sup>. Thus, the number counts variations due to intrinsic clustering and shot-noise is:

$$\frac{\Delta N}{N} \simeq \left[ \bar{w}_2[\theta; z; \mathcal{D}] + \frac{1}{A\mathcal{N}} \right]^{1/2} \quad (3)$$

where  $\bar{w}_2[\theta; z; \mathcal{D}]$  is the angular variance of depth  $\mathcal{D}$  at redshift  $z$ . We next need to quantify the effects of projection and clustering evolution.

### 3 Projection effects

Let us first assume that the 2-pt function  $\xi_2(r_{12})$  does not evolve in co-moving coordinates:  $\xi_2(r_{12}) = \xi_2(x_{12})$ , where  $r_{12} = x_{12}/(1+z)$ . We then have that:

$$\bar{w}_2(\theta) = \int_V d\mathbf{x}_1 d\mathbf{x}_2 \psi(x_1) \psi(x_2) \xi_2(\mathbf{x}_{12}), \quad (4)$$

where  $d\mathbf{x}_i$  is the co-moving volume,  $\psi(x)$  is the normalized probability that a galaxy at a coordinate  $x$  is included in the catalogue and  $V$  is a cone (or pyramid) of radius (or side)  $\theta$  and infinite depth (with solid angle equal to the sample area  $A$ ). In the small angle approximation, *e.g.* when the transverse distances are much smaller than the radial ones, we can relate the angular clustering of samples projected at two different characteristic co-moving depths  $\mathcal{D}_2$  and  $\mathcal{D}_1$  by:

$$\bar{w}_2[\theta; \mathcal{D}_1] = \frac{\mathcal{D}_2}{\mathcal{D}_1} \bar{w}_2[\theta\mathcal{D}_2/\mathcal{D}_1; \mathcal{D}_2]. \quad (5)$$

We take  $\mathcal{D}_2 \simeq 400h^{-1}\text{Mpc}$  as the mean APM depth and  $\mathcal{D}_1 \simeq 2500h^{-1}\text{Mpc}$  as the mean co-moving depth of a typical submm sample (the actual number depends on both the mean redshift and the cosmological parameters, as given by the luminosity distance relation). Thus the curve that fits the APM measurements (solid curve) in Fig.1 must be moved left by a factor  $\mathcal{D}_2/\mathcal{D}_1$  to account for the fact that, at larger radial distances, the same physical length subtends a smaller angle. The APM curve must also be moved down by a factor  $\mathcal{D}_2/\mathcal{D}_1$  because more galaxies are seen in projection at greater radial distances. The resulting prediction in this case, scaled from Eq.[1] to  $\mathcal{D}_1 \simeq 2500h^{-1}\text{Mpc}$  with Eq.[5], is shown as the dotted line in Fig.1. The dotted-dashed line includes the shot-noise contribution in Eq.[3] for a submm  $850\mu\text{m}$  flux limit of 3 mJy, with surface density  $\mathcal{N} = 2000/\text{sq. deg.}$ , which are characteristic of the HDF counts. Note how in this case the variance of the counts are dominated by shot-noise at almost all scales. These predictions agree well with the source-count variations found in our submm simulations of the HDF (see Hughes & Gaztañaga in these proceedings), which also have clustering fixed in co-moving coordinates and the same mean depth.

### 4 The redshift evolution of clustering

We next model the redshift evolution of  $\xi_2$  in proper coordinates  $r_{12} = x_{12}/(1+z)$  as:

$$\xi(r_{12}; z) \simeq (1+z)^{-(3+\epsilon)} \xi(r_{12}; 0) \quad (6)$$

For stable clustering (pattern fixed at proper separations) we have  $\epsilon \simeq 0$  at small scales <sup>2</sup>. For a power-law correlation with slope  $\gamma \simeq 1.7$ , linear theory gives  $\epsilon = \gamma - 1 \simeq 0.7$  and non-linear growth gives  $\epsilon \simeq 1$ . If the clustering is fixed in co-moving coordinates, then  $\epsilon \simeq \gamma - 3 \simeq -1.3$  which produces even less evolution than in the stable clustering regime. This fixed clustering model describes galaxies which are identified with high density-peaks: peaks move less than particles, which results in less evolution. Weak evolution is consistent with the strong clustering observed in Lyman-break galaxies at  $z \simeq 3$ , which is comparable to the clustering of present-day galaxies <sup>3</sup>. The above model of cluster evolution projects as:

$$\bar{w}_2 [ \theta; z_1; \mathcal{D} ] \simeq \left( \frac{1+z_2}{1+z_1} \right)^{3+\epsilon-\gamma} \bar{w}_2 [ \theta; z_2; \mathcal{D} ] \quad (7)$$

where  $\gamma$  varies from  $\simeq 1.6$  over the smaller scales to  $\gamma \simeq 2$  near the exponential break. Here we use  $z_2 \simeq 0.15$  for the APM depth and  $z_1 \simeq 2$  for the depth in sub-mm samples. The resulting predictions, scaled from Eq.[1] to  $\mathcal{D}_1 \simeq 2500h^{-1}\text{Mpc}$ , are shown as the dotted ( $\epsilon = \gamma - 3$ ), short-dashed line ( $\epsilon = 0$ ) and long-dashed lines ( $\epsilon = \gamma - 1$ ) in Fig.1.

## 5 Discussion

In summary, our recipe for the angular variance of number count fluctuations  $(\frac{\Delta N}{N})^2 \equiv \bar{w}_2$  in a galaxy sample of area  $A = \theta^2$ , mean co-moving depth  $\mathcal{D}$  and mean redshift  $z$ , is given by:

$$\bar{w}_2 [ \theta; z; \mathcal{D} ] \simeq \frac{400h^{-1}\text{Mpc}}{\mathcal{D}} \left( \frac{1.15}{1+z} \right)^{3+\epsilon-\gamma} (\theta/\theta_0)^{2\beta} e^{-(\theta/\theta_c)^2} + \frac{1}{\theta^2 \mathcal{N}} \quad (8)$$

where  $\beta \simeq -0.175$ ,  $\theta_c \sim 10.5 \text{ deg.}$ ,  $\theta_0 \simeq 8.7 \times 10^{-3} \text{ deg.}$ ,  $3+\epsilon-\gamma$  is between 0 and 2, depending on clustering evolution, and  $\mathcal{N}$  is the mean number density of sources at the given flux that produces shot-noise fluctuations (*e.g.* Eq.[3]). Several cases for the above model are shown in Fig.1. Assuming the shot-noise is negligible, *e.g.*  $\mathcal{N} \rightarrow \infty$ , to reach a 1% level of fluctuation in  $N$  (lower horizontal line in the figure) we require a sample of about  $A \simeq 6 \text{ sq. deg.}$  for the model with co-moving evolution and about  $A \simeq 1 \text{ sq. deg.}$  for a model with strong clustering evolution. In the submm survey of the HDF <sup>4</sup>, with  $A = 0.001 \text{ sq. deg.}$  (the left vertical line in the Fig.1), we expect  $\Delta N/N \simeq 0.2$  in the case of weak clustering evolution and  $\simeq 0.05$  for the strong evolution case. Thus, in principle, comparing number counts in a few more submm surveys, similar in area to the HDF, would provide a clear discrimination between clustering evolution models.

Nevertheless in small submm surveys the number counts for bright sources will be low, *e.g.*  $N = \theta^2 \mathcal{N} \simeq 3$  for  $S_{850\mu\text{m}} \simeq 3\text{ mJy}$  in the HDF survey <sup>4</sup>, and hence the shot-noise correction dominates and masks any evolution in the clustering. This situation is shown as a dot-dashed line in Fig.1 for the submm HDF survey. In this case, we could still subtract the shot-noise contribution using Eq.[3] although this will introduce large uncertainties. Thus, in the future, it is necessary to extend the surveys to larger areas and/or to lower flux densities in order to have a discriminating measurement of clustering. The Gran Telescopio Milimétrico/Large Millimeter Telescope <sup>6</sup> will be the optimal facility to provide this new generation of deep and wide mm surveys.

## References

1. Gaztañaga, E., *MNRAS* **268**, 913 (1994).
2. Gaztañaga, E., *ApJ* **454**, 561 (1995).
3. Giavalisco, M. *et al*, 1998 *ApJ* **503**, 543 (1998).
4. Hughes, D.H. *et al*, *Nature* **394**, 241 (1998).
5. Maddox, S. J. *et al*, *MNRAS* **242**, 43P (1990).
6. <http://www.lmtgtm.org/>